



HYDROELASTIC VISCOUS OSCILLATIONS IN A CIRCULAR CYLINDRICAL CONTAINER WITH AN ELASTIC COVER

H. F. BAUER

*Institut für Raumfahrttechnik, Universität der Bundeswehr München
85577 Neubiberg, Germany*

AND

M. CHIBA

*Department of Mechanical Engineering, Iwate University
Morioka 020-8551, Japan*

(Received 17 March 1999, and in final form 10 March 2000)

If the surface of a viscous liquid is completely covered by an elastic structure, the hydroelastic frequencies are shifted to a larger magnitude than those obtained with a free surface. It was found that viscosity decreases the oscillation frequencies in comparison to the coupled hydroelastic frequencies of frictionless liquid and that a new phenomenon appears, exhibiting for certain liquid height ranges h/a only aperiodic motion. With increasing angular and radial mode numbers these aperiodic ranges of h/a decrease. Higher modes show larger damping. An increase in the membrane tension decreases the aperiodic region, while an increase in the mass of the membrane increases it.

© 2000 Academic Press

1. INTRODUCTION

IN MODERN TECHNOLOGY the trend toward thinner and lighter structures is predominant. This leads to a high flexibility of the systems, which in many cases involve large capacity containers for liquid or propellant storage, such as in storage tanks or containers in airplanes, missiles, space vehicles, satellites or space stations. Strong interactions of this propellant with the control system and the elastic structure may appear, endangering the integrity of the system and the success of the mission. Thus, shifting these instability frequencies is usually the only way to remedy the troublesome problem. This may be achieved by considering the free liquid surface with a flexible structural member, such as a membrane or a thin elastic plate, with various possible boundary conditions. In this way a coupled frequency system is considered, possibly showing frequencies away from the dangerous one of the original system. It is, of course, mandatory to know the magnitude of the coupled frequencies. The first research activity in this area in recent years, involving a lot of experiments and analyses (Miles 1958; Lindholm *et al.* 1962; Baron & Skalak 1962; Chu 1963; Saleme & Liber 1965; Tsui & Small 1968; Bhuta *et al.* 1964; Bhuta & Koval 1964; Yamaki *et al.* 1984; Bauer *et al.* 1968*a, b*, 1972; Bauer & Siekmann 1969, 1971; Bauer 1970, 1973; Lakis & Paidoussis 1971; Stillman 1973; Jain 1974; Nash *et al.* 1980; Haroun & Housner 1981; Balendra *et al.* 1982) on cylindrical tanks partially filled with frictionless liquid, emphasizes the importance of such hydroelastic investigations. Similar

investigations have been performed for rectangular containers with an elastic liquid surface cover (Bauer 1981). Recently, the coupled frequencies of a circular cylindrical container with an elastic cover and filled with inviscid liquid has been determined by Bauer (1995). For annular liquid systems under zero-gravity conditions the coupled frequencies have also been determined (Bauer 1987).

In what follows, an investigation is presented of the coupled frequencies of a hydroelastic system consisting of a circular cylindrical container, filled with incompressible viscous liquid, the liquid surface of which is covered by an elastic element, such as a flexible membrane or an elastic plate with various boundary conditions. This means that the plate could be clamped or floated with free boundary conditions, be simply supported or guided, such that the rim of the plate would be able to move up and down the wall of the cylinder, exhibiting no shear forces. The case of an elastically supported boundary, where the edge rotation would be opposed by spiral springs having the distributed stiffness (K moment per unit length), will also be mentioned.

2. BASIC EQUATION AND SOLUTION

A circular cylindrical container of diameter $2a$ (Figure 1) is filled to a height h with an incompressible and viscous liquid of density ρ and dynamic viscosity $\bar{\eta}$. The container wall $r = a$ and bottom of the container at $z = -h$ are rigid, while the free surface at $z = 0$ is covered with a flexible membrane or an elastic plate. A list of symbols is given in the Nomenclature (Appendix B). The plate may have various types of attachment to the cylinder wall, such as clamped, simply supported, free, guided, or it may be elastically supported. We assume small displacement and velocities such that the motion of the system has to satisfy the Stokes equations ($v = \bar{\eta}/\rho$),

$$\frac{\partial u}{\partial t} + \frac{1}{\rho} \frac{\partial p}{\partial r} = v \left[\frac{\partial^2 u}{\partial r^2} + \frac{1}{r} \frac{\partial u}{\partial r} - \frac{u}{r^2} + \frac{1}{r^2} \frac{\partial^2 u}{\partial \varphi^2} + \frac{\partial^2 u}{\partial z^2} - \frac{2}{r^2} \frac{\partial v}{\partial \varphi} \right], \tag{1a}$$

$$\frac{\partial v}{\partial t} + \frac{1}{\rho} \frac{\partial p}{r \partial \varphi} = v \left[\frac{\partial^2 v}{\partial r^2} + \frac{1}{r} \frac{\partial v}{\partial r} - \frac{v}{r^2} + \frac{1}{r^2} \frac{\partial^2 v}{\partial \varphi^2} + \frac{\partial^2 v}{\partial z^2} + \frac{2}{r^2} \frac{\partial u}{\partial \varphi} \right], \tag{1b}$$

$$\frac{\partial w}{\partial t} + \frac{1}{\rho} \frac{\partial p}{\partial z} = v \left[\frac{\partial^2 w}{\partial r^2} + \frac{1}{r} \frac{\partial w}{\partial r} + \frac{1}{r^2} \frac{\partial^2 w}{\partial \varphi^2} + \frac{\partial^2 w}{\partial z^2} \right] - g, \tag{1c}$$

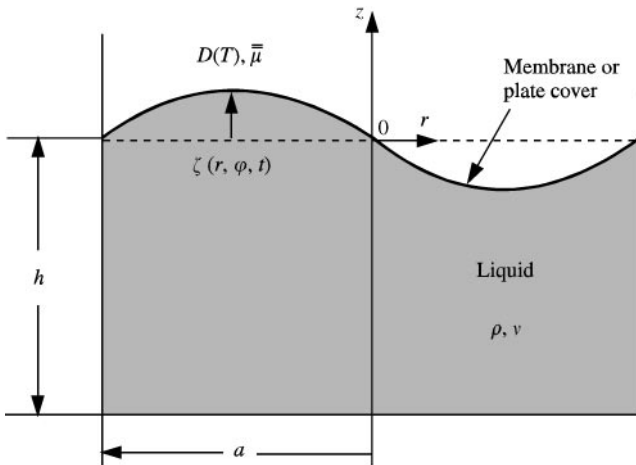


Figure 1. Geometry and coordinate system.

the continuity equation,

$$\frac{\partial u}{\partial r} + \frac{u}{r} + \frac{1}{r} \frac{\partial v}{\partial \varphi} + \frac{\partial w}{\partial z} = 0, \tag{2}$$

and the equation of the elastic cover,

$$T \left[\frac{\partial^2 \zeta}{\partial r^2} + \frac{1}{r} \frac{\partial \zeta}{\partial r} + \frac{1}{r^2} \frac{\partial^2 \zeta}{\partial \varphi^2} \right] = \bar{\mu} \frac{\partial^2 \zeta}{\partial t^2} - \left(p - 2\bar{\eta} \frac{\partial w}{\partial z} \right)_{z=0} \tag{3a}$$

if it is represented by a flexible membrane, or

$$D \left[\frac{\partial^2}{\partial r^2} + \frac{1}{r} \frac{\partial}{\partial r} + \frac{1}{r^2} \frac{\partial^2}{\partial \varphi^2} \right]^2 \zeta + \bar{\mu} \frac{\partial^2 \zeta}{\partial t^2} = \left(p - 2\bar{\eta} \frac{\partial w}{\partial z} \right)_{z=0} \tag{3b}$$

if the covering is by an elastic plate (Leissa 1969). In these equations T is the tension of the membrane, $\zeta(r, \varphi, t)$ the deflection, $\bar{\mu}$ the mass per unit area, $D = E\delta^3/[12(1 - \bar{\nu}^2)]$ the flexural rigidity of the plate with δ as its thickness, $\bar{\nu}$ as Poisson's ratio and E as Young's modulus of elasticity; $\mathbf{v} = u\mathbf{e}_r + v\mathbf{e}_\varphi + w\mathbf{k}$ is the velocity, and the pressure distribution is

$$p(r, \varphi, z, t) = p_o - \rho g z + \bar{p}(r, \varphi, z, t).$$

Actually, the plate exhibits displacement ξ, η and ζ , in the radial, circumferential and axial (normal) direction, respectively. This would require the coupled equations in ξ, η and ζ , and in addition the compatibility conditions, i.e. velocity matching condition between plate/membrane and liquid (adherence and no cavitation), described by

$$\frac{\partial \xi}{\partial t} = u, \quad \frac{\partial \eta}{\partial t} = v \quad \text{and} \quad \frac{\partial \zeta}{\partial t} = w \quad \text{at} \quad z = 0.$$

Assuming that the radial and circumferential deflections are small in comparison with the normal deflection $\zeta(r, \varphi, t)$ results in the boundary conditions at the plate

$$u = v = 0 \quad \text{and} \quad \frac{\partial \zeta}{\partial t} = w \quad \text{at} \quad z = 0. \tag{4}$$

Assuming u, v, w and \bar{p} to be proportional to $e^{im\varphi}e^{st}$, i.e. ($u = e^{st}\sum_m U_m(r, z)e^{im\varphi}$ etc.), we obtain with

$$\phi = U + iV \quad \text{and} \quad \psi = U - iV, \tag{5a}$$

$$U = \frac{1}{2}(\phi + \psi) \quad \text{and} \quad V = \frac{i}{2}(\psi - \phi), \tag{5b}$$

from the stokes equations, equation (1),

$$\frac{\partial^2 \phi}{\partial r^2} + \frac{1}{r} \frac{\partial \phi}{\partial r} - \frac{(m + 1)^2}{r^2} \phi - \frac{s}{v} \phi + \frac{\partial^2 \phi}{\partial z^2} = \frac{1}{\bar{\eta}} \left[\frac{\partial \bar{P}}{\partial r} - \frac{m}{r} \bar{P} \right], \tag{6a}$$

$$\frac{\partial^2 \psi}{\partial r^2} + \frac{1}{r} \frac{\partial \psi}{\partial r} - \frac{(m - 1)^2}{r^2} \psi - \frac{s}{v} \psi + \frac{\partial^2 \psi}{\partial z^2} = \frac{1}{\bar{\eta}} \left[\frac{\partial \bar{P}}{\partial r} + \frac{m}{r} \bar{P} \right], \tag{6b}$$

$$\frac{\partial^2 W}{\partial r^2} + \frac{1}{r} \frac{\partial W}{\partial r} - \frac{m^2}{r^2} W - \frac{s}{v} W + \frac{\partial^2 W}{\partial z^2} = \frac{1}{\bar{\eta}} \frac{\partial \bar{P}}{\partial z}, \tag{6c}$$

and from the continuity equation,

$$\frac{\partial \phi}{\partial r} + \frac{(m + 1)}{r} \phi + \frac{\partial \psi}{\partial r} - \frac{(m - 1)}{r} \psi = -2 \frac{\partial W}{\partial z}. \tag{7}$$

For the solution of this system of coupled partial differential equations we assume a solution of the form

$$\begin{aligned} \phi(r, z) &= A(z) J_{m+1} \left(\varepsilon_{mn} \frac{r}{a} \right), & \psi(r, z) &= -A(z) J_{m-1} \left(\varepsilon_{mn} \frac{r}{a} \right), \\ W(r, z) &= C(z) J_m \left(\varepsilon_{mn} \frac{r}{a} \right), & \bar{P}(r, z) &= D(z) J_m \left(\varepsilon_{mn} \frac{r}{a} \right), \end{aligned} \tag{8}$$

where ε_{mn} are the roots of $J'_m(\varepsilon) = 0$, with which the wall boundary condition

$$u = 0 \quad \text{at} \quad r = a \tag{9}$$

is satisfied. In the representation of equations (5)–(8), the subscript m is omitted for convenience.

From inviscid liquid oscillations, in which only the normal velocity boundary condition $u = 0$ at $r = a$ is satisfied, the radial velocity $u \sim J'_m(\varepsilon_{mn} r/a)$. A glance at the Stokes equations(1a–c) and the continuity equation reveals that the angular velocity $v \sim [1/(\varepsilon_{mn} r/a)] J_m(\varepsilon_{mn} r/a)$, the axial velocity $w \sim J_m(\varepsilon_{mn} r/a)$ and that the pressure distribution $\bar{p} \sim J_m(\varepsilon_{mn} r/a)$. For these reasons equations (8), with the aid of equation (5b) and the recurrence formulas of the Bessel function J_m , yield

$$\begin{aligned} \frac{1}{2} \left[J_{m-1} \left(\varepsilon_{mn} \frac{r}{a} \right) - J_{m+1} \left(\varepsilon_{mn} \frac{r}{a} \right) \right] &= J_m \left(\varepsilon_{mn} \frac{r}{a} \right), \\ \frac{1}{2} \left[J_{m-1} \left(\varepsilon_{mn} \frac{r}{a} \right) + J_{m+1} \left(\varepsilon_{mn} \frac{r}{a} \right) \right] &= \frac{m}{\varepsilon_{mn} r/a} J_m \left(\varepsilon_{mn} \frac{r}{a} \right), \end{aligned}$$

the solutions presented in equation (8). The solution of the above equations (6) and (7) yield the ordinary coupled system of differential equations for A , C and D , i.e.

$$A'' - \mu^2 A = -\frac{\varepsilon_{mn}}{a\bar{\eta}} D, \quad C'' - \mu^2 C = \frac{D'}{\bar{\eta}}, \tag{10}$$

$$\frac{\varepsilon_{mn}}{a} A + C' = 0, \quad \mu^2 \equiv \mu_{mn}^2 = \frac{\varepsilon_{mn}^2}{a^2} + \frac{S}{v}$$

in which $d(\)/dz \equiv (\)'$, $\bar{\mu}_{mn}^2 = \varepsilon_{mn}^2 + S$ and $S \equiv sa^2/\nu$; this gives the solution

$$A(z) = A_{1mn} \cosh \left(\varepsilon_{mn} \frac{z}{a} \right) + A_{2mn} \sinh \left(\varepsilon_{mn} \frac{z}{a} \right) + A_{3mn} \cosh (\mu_{mn} z) + A_{4mn} \sinh (\mu_{mn} z), \tag{11a}$$

$$\begin{aligned} C(z) &= - \left[A_{1mn} \sinh \left(\varepsilon_{mn} \frac{z}{a} \right) + A_{2mn} \cosh \left(\varepsilon_{mn} \frac{z}{a} \right) \right. \\ &\quad \left. + \frac{\varepsilon_{mn}}{\bar{\mu}_{mn}} \left\{ A_{3mn} \sinh \left(\bar{\mu}_{mn} \frac{z}{a} \right) + A_{4mn} \cosh \left(\bar{\mu}_{mn} \frac{z}{a} \right) \right\} \right], \end{aligned} \tag{11b}$$

$$D(z) = \frac{\rho s a}{\varepsilon_{mn}} \left[A_{1mn} \cosh \left(\varepsilon_{mn} \frac{z}{a} \right) + A_{2mn} \sinh \left(\varepsilon_{mn} \frac{z}{a} \right) \right]. \tag{11c}$$

The boundary conditions at the bottom, $z = -h$, are

$$u = v = w = 0 \quad \text{at } z = -h, \tag{11d}$$

and at the elastic cover equation (4)

$$u = v = 0 \quad \text{at } z = 0. \tag{11e}$$

yields

$$A_{3mn} = -A_{1mn}, \tag{12a}$$

$$A_{1mn} \left\{ \cosh\left(\varepsilon_{mn} \frac{h}{a}\right) - \cosh\left(\bar{\mu}_{mn} \frac{h}{a}\right) \right\} - A_{2mn} \sinh\left(\varepsilon_{mn} \frac{h}{a}\right) - A_{4mn} \sinh\left(\bar{\mu}_{mn} \frac{h}{a}\right) = 0, \tag{12b}$$

and

$$A_{1mn} \left\{ \sinh\left(\varepsilon_{mn} \frac{h}{a}\right) - \frac{\varepsilon_{mn}}{\bar{\mu}_{mn}} \sinh\left(\bar{\mu}_{mn} \frac{h}{a}\right) \right\} - A_{2mn} \cosh\left(\varepsilon_{mn} \frac{h}{a}\right) - A_{4mn} \frac{\varepsilon_{mn}}{\bar{\mu}_{mn}} \cosh\left(\bar{\mu}_{mn} \frac{h}{a}\right) = 0, \tag{12c}$$

for given m and $n = 1, 2, 3, \dots$

2.1. MEMBRANE COVER

If the liquid surface is covered by a flexible membrane, we have to solve equation (3a) with the boundary condition

$$\zeta = 0 \quad \text{at } r = a. \tag{13a}$$

This means that

$$\zeta(r, \varphi, t) = \sum_{m=0}^{\infty} \bar{\zeta}_m(r) e^{im\varphi} e^{st}, \tag{13b}$$

$$\begin{aligned} \frac{d^2 \bar{\zeta}_m}{dr^2} + \frac{1}{r} \frac{d \bar{\zeta}_m}{dr} - \frac{m^2}{r^2} \bar{\zeta}_m - \left(\frac{\bar{\mu}s^2}{T} + \frac{\rho g}{T} \right) \bar{\zeta}_m &= \frac{2\bar{\eta}}{T} \sum_{n=1}^{\infty} C'_{mn}(0) J_m\left(\varepsilon_{mn} \frac{r}{a}\right) \\ &- \frac{1}{T} \sum_{n=1}^{\infty} D_{mn}(0) J_m\left(\varepsilon_{mn} \frac{r}{a}\right) - \frac{P_0}{T}, \end{aligned} \tag{14}$$

which yields the solution

$$\bar{\zeta}_m(r) = A_{0m} I_m\left(\beta \frac{r}{a}\right) + \frac{\rho s a^3}{T} \sum_{n=1}^{\infty} \frac{A_{1mn} J_m(\varepsilon_{mn} r/a)}{\varepsilon_{mn} (\varepsilon_{mn}^2 - \beta^2)} + P_0^*, \tag{15}$$

where

$$\beta^2 \equiv \frac{a^2(\bar{\mu}s^2 + \rho g)}{T} \quad \text{and} \quad S \equiv \frac{sa^2}{\nu}, \quad \mu^* \equiv \frac{\bar{\mu}}{\rho a}.$$

Boundary condition (13a) with $\bar{A}_{jmn} \equiv A_{jmn}a^2/v$ and $P_0^* = 0$ for $m \neq 0$ gives

$$A_{0m}I_m(\beta) + \frac{S}{T^*} \sum_{n=1}^{\infty} \frac{\bar{A}_{1mn} J_m(\epsilon_{mn})}{\epsilon_{mn}[\epsilon_{mn}^2 - ((\bar{\mu}/\rho a)S^2 + g^*)/T^*]} = 0, \tag{16}$$

where $g^* \equiv ga^3/v^2$ and $T^* \equiv Ta/\rho v^2$. Expanding $I_m(\beta r/a)$ into a Bessel-Fourier series, i.e. ($m \neq 0$)

$$I_m\left(\beta \frac{r}{a}\right) = 2\beta \sum_{n=1}^{\infty} \frac{\epsilon_{mn}^2 I_m(\beta) J_m(\epsilon_{mn} r/a)}{J_m(\epsilon_{mn}) (\epsilon_{mn}^2 + \beta^2)(\epsilon_{mn}^2 - m^2)}, \tag{17}$$

introducing it into equation (15) and comparing with the results obtained from the compatibility condition

$$\frac{\partial \zeta}{\partial t} = w \quad \text{at } z = 0 \tag{18}$$

with

$$\zeta(r, \phi, t) = e^{st} \sum_{m=0}^{\infty} \sum_{n=1}^{\infty} \zeta_{mn} J_m\left(\epsilon_{mn} \frac{r}{a}\right) e^{im\phi}$$

yields

$$\zeta_{mn} = -\frac{1}{S} \left[\bar{A}_{2mn} + \frac{\epsilon_{mn}}{\sqrt{\epsilon_{mn}^2 + S}} \bar{A}_{4mn} \right]. \tag{19}$$

By comparing the coefficients of $J_m(\epsilon_{mn} r/a)$, we obtain the equations

$$2\beta A_{0m} \frac{\epsilon_{mn}^2 I'_m(\beta)}{J_m(\epsilon_{mn})(\epsilon_{mn}^2 - m^2)} + \frac{S}{T^* \epsilon_{mn}} \frac{(\epsilon_{mn}^2 + \beta^2)}{(\epsilon_{mn}^2 - \beta^2)} \bar{A}_{1mn} + \frac{1}{S} \left[\bar{A}_{2mn} + \frac{\epsilon_{mn}}{\sqrt{\epsilon_{mn}^2 + S}} \bar{A}_{4mn} \right] (\epsilon_{mn}^2 + \beta^2) = 0, \tag{20}$$

for given $m \neq 0$ and $n = 1, 2, \dots$

The vanishing coefficient determinant of the $(3n + 1)$ equations (12b, c), (16) and (20) represents the frequency equation for the determination of the damped (complex) coupled frequencies of the membrane-viscous liquid system. If the determinant is truncated to a finite order we obtain the approximate values of the lower frequencies.

For *axisymmetric* oscillations, $m = 0$, the expansion of $I_0(\beta r/a)$ is given by

$$I_0\left(\beta \frac{r}{a}\right) = \frac{2}{\beta} I_1(\beta) + 2\beta \sum_{n=1}^{\infty} \frac{I_1(\beta) J_0(\epsilon_{0n} r/a)}{J_0(\epsilon_{0n}) (\epsilon_{0n}^2 + \beta^2)}, \tag{21}$$

with $P_0^* \neq 0$ for $m = 0$ and the above expansion procedure, we obtain the additional equation

$$\frac{2}{\beta} I_1(\beta) A_{00} + P_0^* = 0 \tag{22a}$$

and

$$2\beta \frac{I_1(\beta)}{J_0(\epsilon_{0n})} A_{00} + \frac{S}{T^* \epsilon_{0n}} \frac{(\epsilon_{0n}^2 + \beta^2)}{(\epsilon_{0n}^2 - \beta^2)} \bar{A}_{10n} + \frac{1}{S} \left[\bar{A}_{20n} + \frac{\epsilon_{0n}}{\sqrt{\epsilon_{0n}^2 + S}} \bar{A}_{40n} \right] (\epsilon_{0n}^2 + \beta^2) = 0. \tag{22b}$$

The vanishing determinant of the $(3n + 2)$ equations (22a, b), (12b, c) and (16) is the axisymmetric frequency equation. It may be noticed that $\beta^2 \equiv (\mu^*S^2 + g^*)/T^*$ and that the volume-preserving condition $\int_0^a \zeta(r, t) r dr = 0$ is satisfied by equation (22a).

2.2. PLATE COVER CASES

If the free liquid surface at $z = 0$ is covered by an elastic plate, then equation (3b) has to be satisfied. We may distinguish different boundary conditions at $r = a$:

clamped: $\zeta = 0$ and $\frac{\partial \zeta}{\partial r} = 0$ at $r = a$; (23)

simply supported: $\zeta = 0, M_r = -D \left[\frac{\partial^2 \zeta}{\partial r^2} + \bar{\nu} \left(\frac{1}{r} \frac{\partial \zeta}{\partial r} + \frac{1}{r^2} \frac{\partial^2 \zeta}{\partial \varphi^2} \right) \right] = 0$ at $r = a$; (24)

free: $M_r = 0$ and $V_r = -D \frac{\partial}{\partial r} \left\{ \frac{\partial^2 \zeta}{\partial r^2} + \frac{1}{r} \frac{\partial \zeta}{\partial r} + \frac{1}{r^2} \frac{\partial^2 \zeta}{\partial \varphi^2} \right\} - \frac{D}{r} (1 - \bar{\nu}) \frac{\partial}{\partial r} \left(\frac{1}{r} \frac{\partial^2 \zeta}{\partial \varphi^2} \right) = 0$ at $r = a$; (25)

guided: $\frac{\partial \zeta}{\partial r} = 0$ and $V_r = 0$ at $r = a$; (26)

elastically supported: $M_r = K \frac{\partial \zeta}{\partial r}$ and $V_r = 0$ at $r = a$; (27)

where $\bar{\nu}$ is Poisson’s ratio and the edge rotation is opposed by torsional springs having a distributed stiffness K (moment per unit length). Equations (1), (2), (3b), (11d, e) and (18), with one of the above boundary conditions, (23)–(27), constitute the hydroelastic problem for a container filled with viscous liquid and a plate cover.

If the plate is *clamped* at $r = a$, we have to apply the boundary condition (23). The solution of the equation of the plate,

$$\left(\frac{d^2}{dr^2} + \frac{1}{r} \frac{d}{dr} - \frac{m^2}{r^2} \right)^2 \bar{\zeta}_m + \left(\frac{\bar{\mu}S^2 + \rho g}{D} \right) \bar{\zeta}_m = \frac{\rho sa}{D} \sum_{n=1}^{\infty} A_{1mn} J_m \left(\varepsilon_{mn} \frac{r}{a} \right) + \frac{p_0}{D}, \tag{28}$$

produces the solution $(\alpha^2 = (\mu^*S^2 + g^*)/D^*, g^* \equiv ga^3/v^2)$

$$\bar{\zeta}_m(r) = \bar{A}_{0m} I_m \left(\alpha \frac{r}{a} \right) + \bar{B}_{0m} J_m \left(\alpha \frac{r}{a} \right) - \frac{\rho sa^5}{D} \sum_{n=1}^{\infty} \frac{A_{1mn} J_m(\varepsilon_{mn} r/a)}{\varepsilon_{mn} (\varepsilon_{mn}^4 + \alpha^4)}, \tag{29}$$

where $D^* = D/\rho v^2 a$. Boundary conditions (23) yield

$$\bar{A}_{0m} I_m(\alpha) + \bar{B}_{0m} J_m(\alpha) - \frac{S}{D^*} \sum_{n=1}^{\infty} \frac{\bar{A}_{1mn} J_m(\varepsilon_{mn})}{\varepsilon_{mn} (\varepsilon_{mn}^4 + \alpha^4)} = 0 \tag{30}$$

and

$$\bar{A}_{0m} I'_m(\alpha) + \bar{B}_{0m} J'_m(\alpha) = 0. \tag{31}$$

Expanding I_m and J_m into Bessel–Fourier series

$$I_m \left(\alpha \frac{r}{a} \right) = 2\alpha \sum_{n=1}^{\infty} \frac{\varepsilon_{mn}^2 I'_m(\alpha) J_m(\varepsilon_{mn} r/a)}{J_m(\varepsilon_{mn}) (\varepsilon_{mn}^2 + \alpha^2) (\varepsilon_{mn}^2 - m^2)}$$

and

$$J_m \left(\alpha \frac{r}{a} \right) = 2\alpha \sum_{n=1}^{\infty} \frac{\varepsilon_{mn}^2 J'_m(\alpha) J_m(\varepsilon_{mn} r/a)}{J_m(\varepsilon_{mn})(\varepsilon_{mn}^2 - \alpha^2)(\varepsilon_{mn}^2 - m^2)},$$

and introducing them into the displacement equation (29), after comparison with the results from the kinematic condition (18), yields finally

$$2\alpha \bar{A}_{0n} \frac{\varepsilon_{mn}^2 J'_m(\alpha)}{(\varepsilon_{mn}^2 + \alpha^2)} + 2\alpha \bar{B}_{0n} \frac{\varepsilon_{mn}^2 J'_m(\alpha)}{(\varepsilon_{mn}^2 - \alpha^2)} - \frac{S}{D^* \varepsilon_{mn}} \bar{A}_{1mn} \frac{J_m(\varepsilon_{mn})(\varepsilon_{mn}^2 - m^2)}{(\varepsilon_{mn}^4 + \alpha^4)} + \frac{1}{S} \left[\bar{A}_{2mn} + \frac{\varepsilon_{mn}}{\sqrt{\varepsilon_{mn}^2 + S}} \bar{A}_{4mn} \right] (\varepsilon_{mn}^2 - m^2) J_m(\varepsilon_{mn}) = 0, \tag{32}$$

for $n = 1, 2, \dots$ and for $m \neq 0$. Equations (30)–(32) and (12b, c) represent $(3n + 2)$ homogeneous algebraic equations, of which the vanishing determinant is the frequency equation for the damped natural frequencies $m \neq 0$ of the hydroelastic system.

For axisymmetric oscillation ($m = 0$) the expansions of I_0 and J_0 are given by

$$I_0 \left(\alpha \frac{r}{a} \right) = \frac{2}{\alpha} I_1(\alpha) + 2\alpha \sum_{n=1}^{\infty} \frac{I_1(\alpha) J_0(\varepsilon_{0n} r/a)}{J_0(\varepsilon_{0n})(\varepsilon_{0n}^2 + \alpha^2)}$$

and

$$J_0 \left(\alpha \frac{r}{a} \right) = \frac{2}{\alpha} J_1(\alpha) + 2\alpha \sum_{n=1}^{\infty} \frac{J_1(\alpha) J_0(\varepsilon_{0n} r/a)}{J_0(\varepsilon_{0n})(\varepsilon_{0n}^2 + \alpha^2)},$$

which, when introduced in the solution of equation (28), i.e.

$$\bar{\zeta}_0(r) = \bar{A}_{00} I_0 \left(\alpha \frac{r}{a} \right) + \bar{B}_{00} J_0 \left(\alpha \frac{r}{a} \right) - \frac{S}{D^*} \sum_{n=1}^{\infty} \frac{\bar{A}_{10n} J_0(\varepsilon_{0n} r/a)}{(\varepsilon_{0n}^4 + \alpha^4)} + P_0^* \tag{33}$$

yield

$$2 \bar{A}_{00} I_0(\alpha) + 2 \bar{B}_{00} J_0(\alpha) + \alpha P_0^* = 0 \tag{34}$$

and

$$2\alpha \frac{I_1(\alpha)}{(\varepsilon_{0n}^2 + \alpha^2)} \bar{A}_{00} + 2\alpha \frac{J_1(\alpha)}{(\varepsilon_{0n}^2 - \alpha^2)} \bar{B}_{00} - \frac{S J_0(\varepsilon_{0n})}{D^*(\varepsilon_{0n}^4 + \alpha^4)} \bar{A}_{10n} + \frac{J_0(\varepsilon_{0n})}{S} \left[\bar{A}_{20n} + \frac{\varepsilon_{0n}}{\sqrt{\varepsilon_{0n}^2 + S}} \bar{A}_{40n} \right] = 0 \tag{35}$$

for $n = 1, 2, \dots$. Equations (12b, c) for $m = 0$, equations (34) and (35) and the boundary conditions of the plate at $r = a$

$$I_0(\alpha) \bar{A}_{00} + J_0(\alpha) \bar{B}_{00} - \frac{S}{D^*} \sum_{m=1}^{\infty} \frac{J_0(\varepsilon_{0n})}{(\varepsilon_{0n}^4 + \alpha^4)} \bar{A}_{10n} + P_0^* = 0 \tag{36a}$$

and

$$I_1(\alpha) \bar{A}_{00} - J_1(\alpha) \bar{B}_{00} = 0 \tag{36b}$$

yield $(3n + 3)$ equations, of which the vanishing determinant represents the frequency equation.

For other boundary conditions the procedure for the solution of the coupled complex frequencies is quite similar to that presented above for a clamped plate.

3. NUMERICAL EVALUATIONS AND CONCLUSIONS

Some of the previously obtained analytical results have been evaluated numerically. This was performed for a membrane cover (Figure 1) in axisymmetric as well as asymmetric motion. In this case, vibration characteristics of the present viscous liquid–membrane coupled system are governed by the following system parameters: tension parameter $T^* \equiv Ta/\rho v^2$, gravitational parameter $g^* \equiv ga^3/v^2$, density ratio $\mu^* \equiv \bar{\mu}/\rho a$, liquid height ratio h/a , and vibration mode $(m, n) = (\text{circumferential, radial})$ wavenumber. The above solution is especially of importance for small liquid height ratios h/a , for which most of the liquid participates in the motion, and for which the adhesive effect of the container bottom contributes a major part to the damped motion. This is due to the fact that the wave motion penetrates only to a depth of the order of about one wavelength. For large liquid height ratios, the lower part of the liquid merely performs a rigid-body motion. This suggests that for such a case the adhesive conditions at the container bottom will produce only a small effect on the overall damping of the liquid, and that in such a case the liquid damping is mainly due to the effects of internal damping. For large h/a values the adhesive wall conditions $v = w = 0$ at $r = a$ will be of paramount influence on the damping behaviour of the liquid. These cases would require a different approach to the solution, in which $v = w = 0$ at the container wall may no longer be neglected.

In previous investigations (Bauer & Eidel 1997a, b) for a viscous liquid in a rigid container with a free liquid surface, the results show the important fact that, for small liquid heights h/a , the liquid is no longer capable of performing damped oscillations, thus exhibiting only an aperiodic motion, if disturbed. The decrease of the surface tension parameter $\sigma^* \equiv \sigma a/\rho v^2$ increases this aperiodic region and decreases the decay magnitude and oscillation frequency for h/a values above the aperiodic region. With increasing gravity parameter $g^* \equiv ga^3/v^2$ the aperiodic region decreases further, while in the oscillation region the decay magnitude as well as the oscillation frequency increases. Higher modes have been shown to exhibit significantly stronger decay. For an infinite region $0 \leq r < \infty$, an aperiodic region exists for small wavelength $\lambda \ll 1$ as well as for very large wavelength $\lambda \gg 1$, which decreases with increasing σ^* and increasing g^* .

If the free liquid surface is covered by a flexible structure we have found that the region of aperiodicity is much larger than for a liquid without such a cover. In the numerical calculations, the number of unknown parameters n in the equations was taken to be three (terms), which is the same number used in equation (17) for the Bessel–Fourier series.

In Figure 2 we show the uncoupled and coupled frequencies of the axisymmetric motion $m = 0$ of the membrane–liquid system as a function of the liquid height ratio h/a . The dashed curves represent the coupled frequencies of the system for nonviscous liquid, while the dotted curve is the uncoupled membrane frequency $\omega_{01}^{*(m)}$. The solid line curves represent the complex coupled frequency of the viscous system, in which the thin solid line shows the decay magnitude $-\delta \equiv -\Re e S$ and the thick solid line shows the oscillation frequency $\omega \equiv \Im m S$. First of all, we notice, that higher modes $m = 0; n = 3, 4$ show a larger decay magnitude, meaning that they are damped out much faster than the fundamental mode $m = 0, n = 2$. With a decrease in the liquid height, the oscillation frequency ω decreases, while the decay magnitude ($-\delta$) increases, indicating a faster decay. For frictionless liquid, which exhibits for all liquid height ratios h/a oscillatory behaviour, we detect a larger oscillation frequency. As may be noticed, the mode $m = 0$ and $n = 1$ does not exist, since the liquid would then not satisfy the continuity equation, i.e. the volume preserving condition.

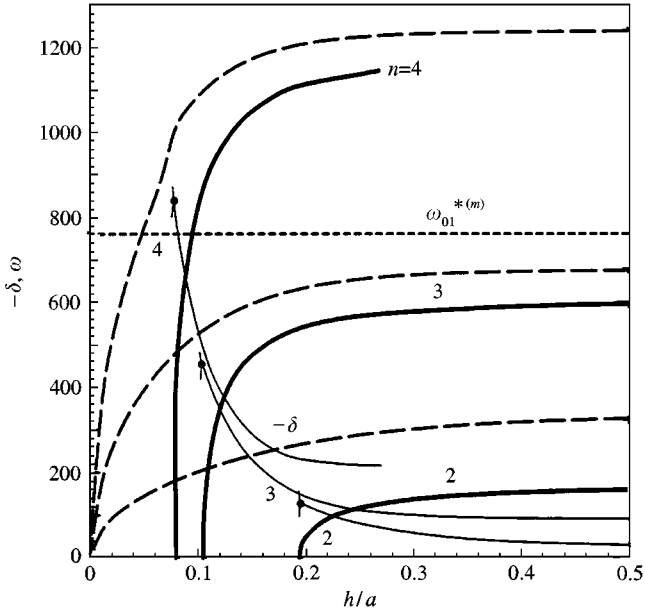


Figure 2. Coupled and uncoupled frequencies of axisymmetric motion for $m = 0$; $T^* = 10^3$, $g^* = 10^4$ and $\mu^* = 10^{-2}$: ----, inviscid coupled frequencies; - · - · - ·, uncoupled membrane frequency $\omega_{01}^{*(m)}$; ·, double roots S_{0n} ($n = 2, 3, 4$).

We detect in Figure 2 that for $m = 0$, $n = 2$ the aperiodic region is located below $h/a \approx 0.195$, while the mode $n = 3$ exhibits a smaller region $h/a \leq 0.105$. The axisymmetric mode $m = 0$, $n = 4$ is in the range $0 \leq h/a < 0.080$ performing only an aperiodic (non-oscillatory) motion. At the decay values $-\delta$, we have emphasized by a dot, the location of the double root, where the oscillation ceases to exist. It may be remarked that the course of the two aperiodic roots in these ranges smaller than $(h/a)_{\text{double root}}$ are not presented. One of them will exhibit a large magnitude (strong decay), while the other will show a smaller value (weaker) decay. The contribution of both, however, will disappear as time goes on. In Figure 3 we represent only the oscillatory frequency of the hydroelastic system, where the dash-dotted lines are the uncoupled natural frequencies of the liquid $\omega_{0j}^{*(l)}$, $j = 1, 2, 3$. The membrane frequency $\omega_{01}^{*(m)}$ is shown as the dotted line. Figure 4 just shows the case of the coupled complex frequency for $m = 0$, $n = 2$ versus the height ratio h/a .

The results for the asymmetric modes $m = 1$ (circumferential nodal line at $\varphi = \pm \pi/2$) and radial modes $n = 1, 2, 3$ are presented in Figure 5 for $T^* \equiv Ta/\rho v^2 = 10^3$, $g^* \equiv ga^3/v^2 = 10^4$, and $\mu^* \equiv \bar{\mu}/\rho a = 10^{-2}$. In the liquid height range presented, $0 \leq h/a \leq 0.5$, only aperiodic motion is possible for the radial mode $n = 1$. The radial mode $n = 2$ exhibits in $0 \leq h/a < 0.135$ an aperiodic motion, while for $n = 3$ this range will be below $h/a \approx 0.09$. In Figure 5, we have again indicated the location of the double roots, S_{1n} ($n = 2, 3$). At this height ratio location h/a the mode ceases to oscillate. For smaller values h/a two negative real roots S appears (not shown in the figure) which indicate that only aperiodic motion is possible. The double root for the mode $m = n = 1$ is outside the range of this figure. The aperiodic branches are not shown.

For the circumferential mode $m = 2$ with two radial nodal lines, one at $\varphi = (\pi/4, 5\pi/4)$ and the other at $\varphi = (3\pi/4, 7\pi/4)$, the numerical results are shown in Figure 6 for the same parameters T^* , g^* and μ^* . Again we notice that the mode $m = 2$, $n = 1$, if disturbed, is only able to perform an aperiodic motion, for the total indicated range $0 \leq h/a \leq 0.5$. The two

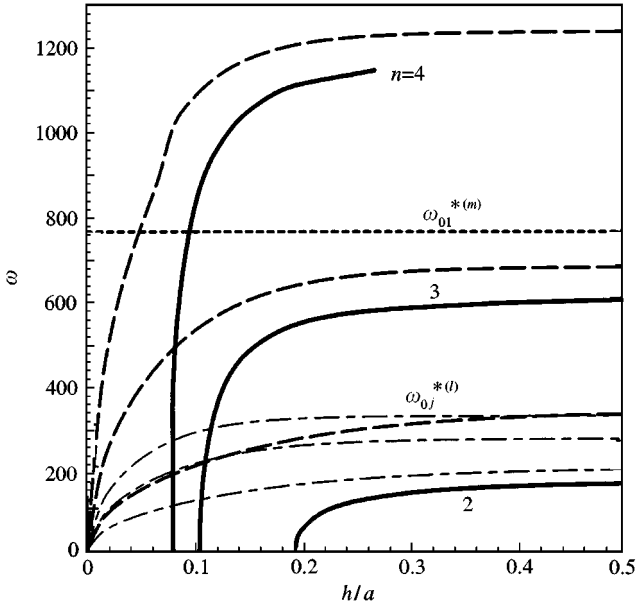


Figure 3. Coupled and uncoupled oscillation frequencies of axisymmetric motion for $m = 0$; $T^* = 10^3$, $g^* = 10^4$ and $\mu^* = 10^{-2}$: ----, inviscid coupled frequencies; - - - - -, uncoupled liquid frequency $\omega_{0j}^{*(l)}$; - · - · - ·, uncoupled membrane frequency $\omega_{01}^{*(m)}$.

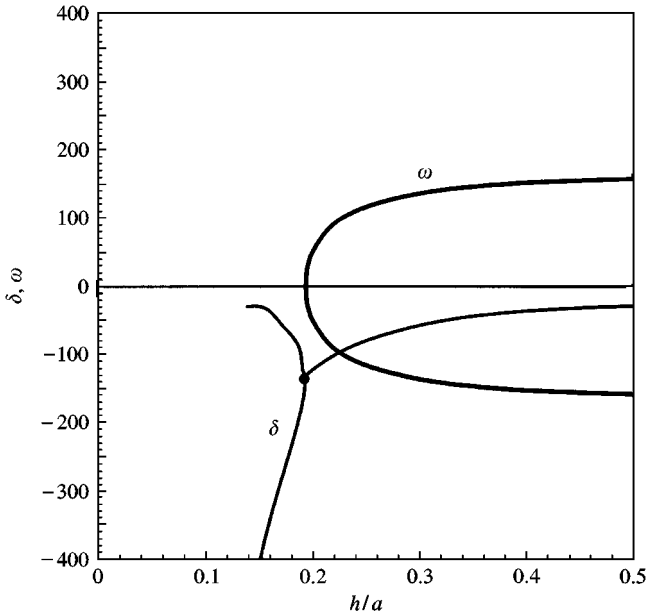


Figure 4. Coupled complex frequency for axisymmetric motion for $m = 0$, $n = 2$; $T^* = 10^3$, $g^* = 10^4$ and $\mu^* = 10^{-2}$.

aperiodic branches are not presented in the figure. For the radial modes $n = 2$ and 3 we notice an aperiodic range for $h/a < 0.108$ and $h/a < 0.08$, respectively.

For higher circumferential modes m the lowest radial mode $n = 1$ becomes finally oscillatory in the range $0 \leq h/a \leq 0.5$. For $m = 3$ (Figure 7) the system performs a decaying

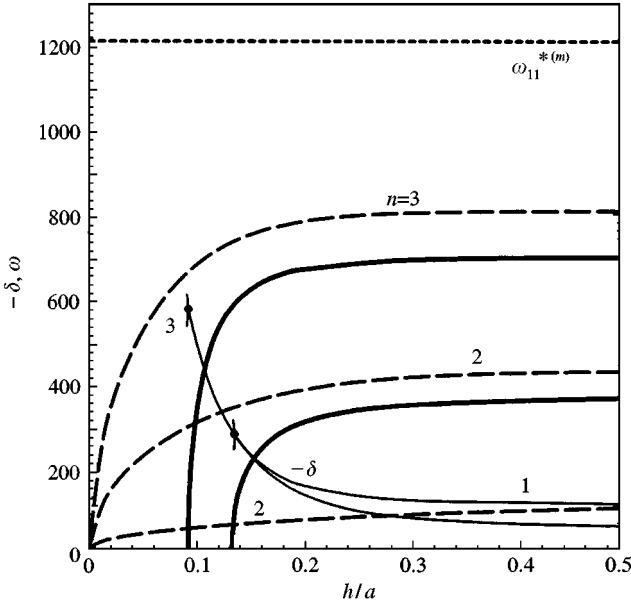


Figure 5. Coupled complex frequency for asymmetric motion for $m = 1$; $T^* = 10^3$, $g^* = 10^4$ and $\mu^* = 10^{-2}$; ----, inviscid coupled frequencies; - - - - -, uncoupled membrane frequency $\omega_{11}^{*(m)}$; *, double roots S_{1n} ($n = 2, 3$).

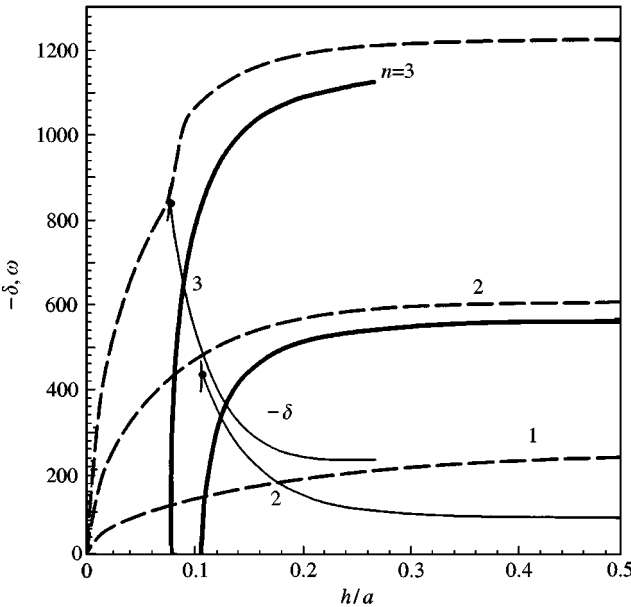


Figure 6. Coupled complex frequency for mode $m = 2$; $T^* = 10^3$, $g^* = 10^4$ and $\mu^* = 10^{-2}$; ----, inviscid coupled frequencies; *, double roots S_{2n} ($n = 2, 3$).

oscillation for a liquid height ratio $h/a > 0.16$. The second radial mode $n = 2$ exhibits larger decay, larger oscillation frequency and a small aperiodic range $0 \leq h/a < 0.093$. This aperiodic range decreases further to values $0 \leq h/a < 0.073$ for the mode $m = 3, n = 3$.

For better interpretation of the vibration modes in Figure 8 are shown the mode shapes for axisymmetric motion $m = 0$. We notice that mode shape of the vibration mode $m = 0, n = 2$

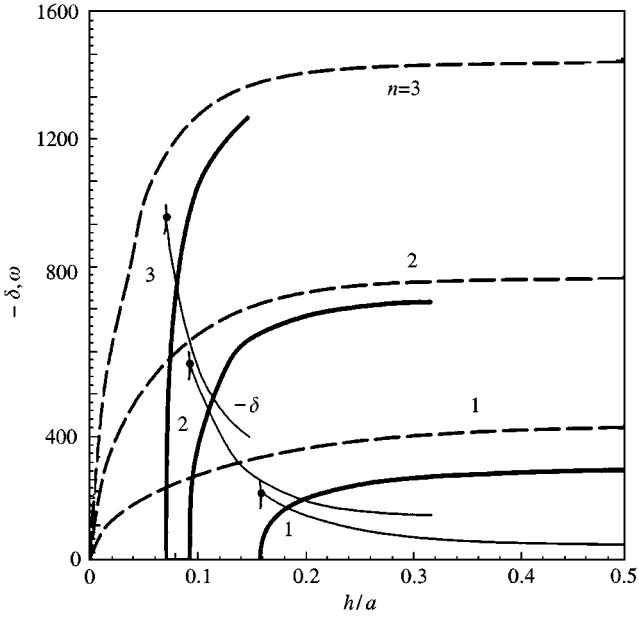


Figure 7. Coupled complex frequency for mode $m = 3$; $T^* = 10^3$, $g^* = 10^4$ and $\mu^* = 10^{-2}$; ----, inviscid coupled frequencies; ·, double roots S_{3n} ($n = 1, 2, 3$).

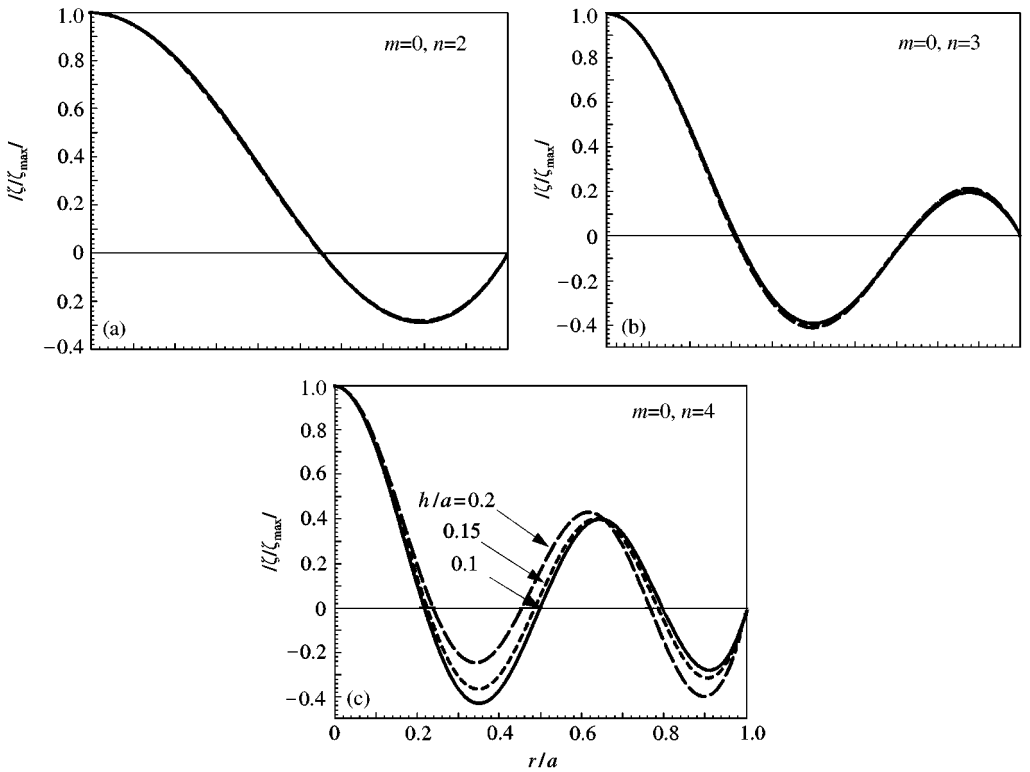


Figure 8. Vibration modes $m = 0$; $T^* = 10^3$, $g^* = 10^4$ and $\mu^* = 10^{-2}$; (a) $n = 2$; (b) $n = 3$; (c) $n = 4$.

exhibits hardly any difference for the treated liquid height ratios $h/a = 0.1, 0.15, 0.2$. For the mode $m = 0, n = 3$ we observe already small differences, while for mode $m = 0, n = 4$ the differences become quite obvious. With increasing liquid height ratio h/a , the mode shape exhibits larger values for the larger h/a -value close to the wall, while towards the centre line $r = 0$ it is smaller than those for smaller liquid height ratio.

Similar results are given in Figure 9 for $m = 1, 2$ and 3 , respectively. For $h/a = 0.4$ [Figure 9(a)] the mode shapes of the modes $m = 1, 2, 3, n = 1$ exhibit no difference, while for smaller h/a -values distinct shifting of extreme values and nodal lines appear [Figure 9(b, c)].

For a deeper insight into the morphology of the roots of the motion of the hydroelastic system, we have determined the double-roots as a function of circumferential modal number m , radial modal number n and the liquid height ratio h/a for the range $0 \leq h/a \leq 0.2$ (Figure 10). These results indicate where the system ceases to oscillate, i.e. where it is only capable to perform an aperiodic motion. It may be seen that the double-root of the mode $n = 1$ is not in the ranges of h/a and $m < 2$ presented, and one may also assume from the slope of the curve for $n = 1$, that $m = 0, n = 1$ will never reach an intersection with the ordinate h/a , i.e. that this mode will not exist, as we know from the volume preserving condition (Figure 8).

In Figure 10, we also detect that the aperiodic region is exhibiting decreased magnitude for a higher membrane tension parameter $T^* = 10^4$. Since the aperiodic region represents a new and interesting phenomenon in the coupled liquid-structure system, we have devoted a little more time to the evaluation of its magnitude depending upon the various parameters

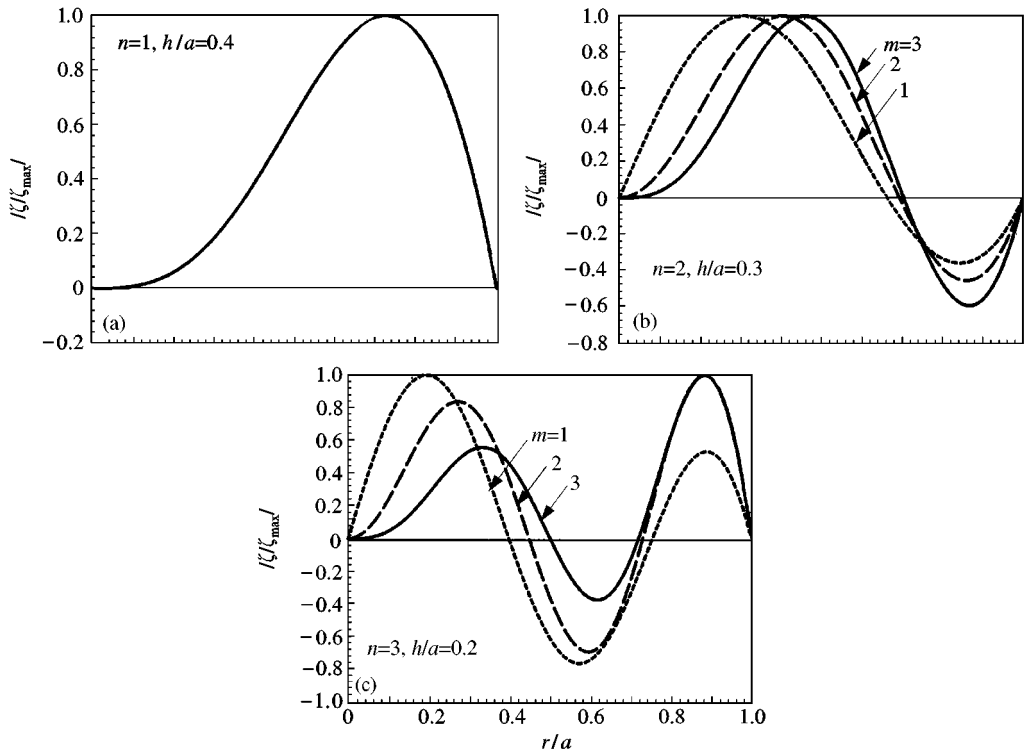


Figure 9. Vibration modes $m \neq 0$; $T^* = 10^3, g^* = 10^4$ and $\mu^* = 10^{-2}$; (a) $n = 1, h/a = 0.4$; (b) $n = 2, h/a = 0.3$; (c) $n = 3, h/a = 0.2$.

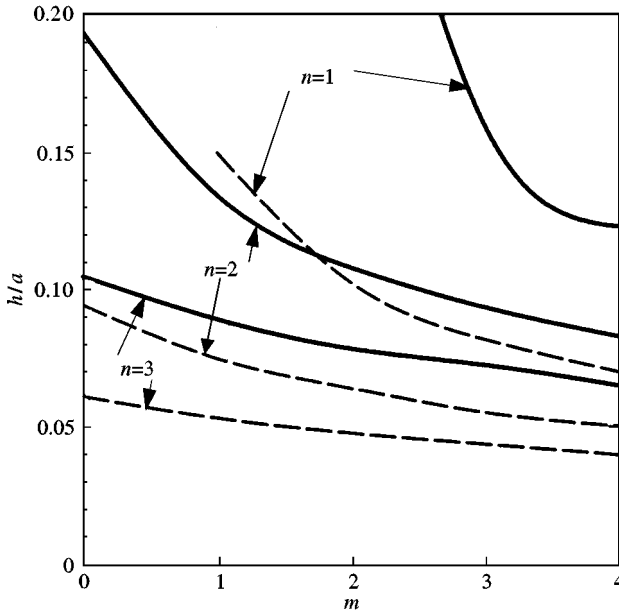


Figure 10. Complex double root, below which only aperiodic motion is possible (for modes $m = 0, 1, 2, 3, 4$), $g^* = 10^4, \mu^* = 10^{-2}$: —, $T^* = 10^3$; ----, $T^* = 10^4$.

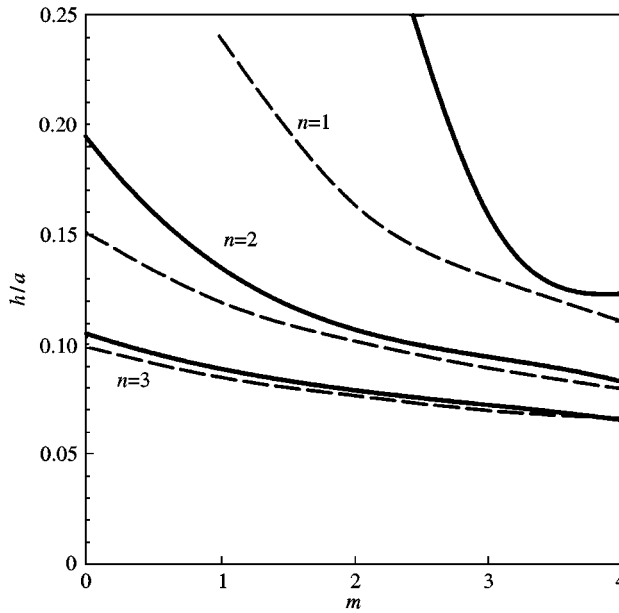


Figure 11. Complex double root, below which only aperiodic motion is possible (for modes $m = 0, 1, 2, 3, 4$), $T^* = 10^3, \mu^* = 10^{-2}$; ----, $g^* = 10^3$; —, $g^* = 10^4$.

of the system, the circumferential mode numbers m and the radial mode numbers n . We notice first of all that the region of aperiodic motion decreases with an increase of both the circumferential mode number m and the radial mode number n . In addition, an increase in the membrane tension reduces the range of aperiodicity. The influence of the gravity parameter $g^* \equiv ga^3/\nu^2$ is presented in Figure 11 for $g^* = 10^3$ and 10^4 . The results show, for a membrane tension parameter of $T^* = 10^3$ and mass parameter $\mu^* = 0.01$, that the

increase in g^* increases the aperiodic region, which is more pronounced for lower radial modes n .

The influence of the mass parameter $\mu^* \equiv \bar{\mu}/\rho a$ upon the magnitude of the aperiodic region is presented in Figure 12, for $T^* = 10^3$, $g^* = 10^3$ and $\mu^* = 0.01$ and 0.05 . It shows that with increasing μ^* the aperiodic region increases for all modes.

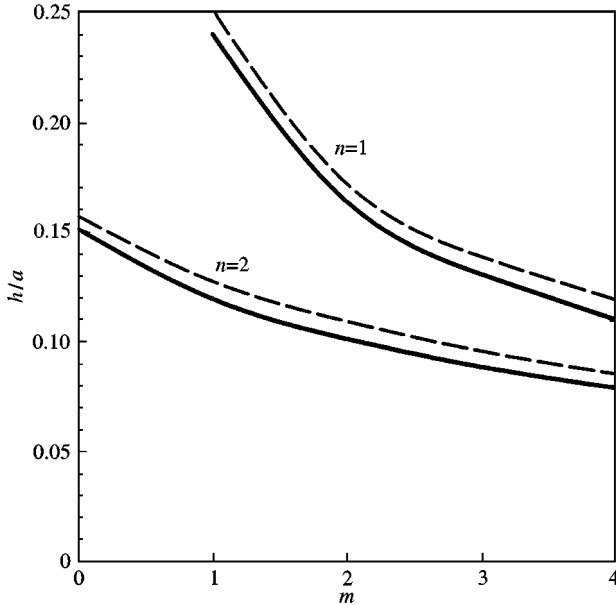


Figure 12. Complex double root, below which only aperiodic motion is possible (for modes $m = 0, 1, 2, 3, 4$), $T^* = 10^3, g^* = 10^3$; —, $\mu^* = 0.01$; ----, $\mu^* = 0.05$.

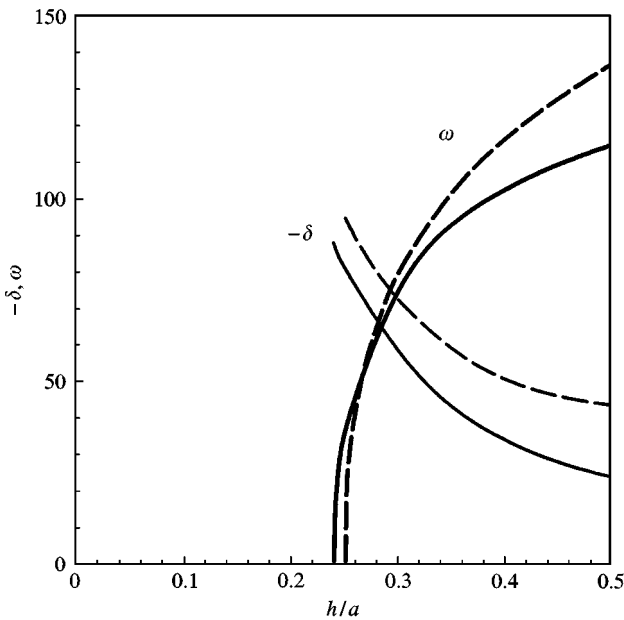


Figure 13. Coupled complex frequency for mode $m = 1, n = 1$; $T^* = 10^3, g^* = 10^3$; —, $\mu^* = 0.01$; ----, $\mu^* = 0.05$.

Finally, we investigated the effect of increasing mass parameter μ^* upon the fundamental damped frequency for $T^* = 10^3$, $g^* = 10^3$ and the mode $m = 1$, $n = 1$. It was found that essentially an increase in the mass parameter $\mu^* \equiv \bar{\mu}/\rho a$ yields an increase of the oscillation frequency and an increase of the decay magnitude (Figure 13).

4. CONCLUSION

From the above results one may conclude the following.

(a) Increasing the mode number results in a decrease in the aperiodic range for small liquid height ratio h/a . This is also true for the circumferential mode number m as well as for radial mode number n .

(b) The effect of viscosity is to decrease the oscillation frequency in comparison with the coupled hydroelastic frequencies of frictionless liquid.

(c) Decreasing liquid height ratio h/a increases the decay magnitude and decreases the oscillation frequency. Higher modes exhibit stronger damping and disappear as time goes on.

(d) An increase in the membrane tension parameter T^* decreases the aperiodic region considerably.

(e) An increase in the gravity parameter $g^* \equiv ga^3/v^2$ increases the aperiodic region, the increase being more pronounced for lower modes.

(f) An increase in the mass parameter $\mu^* \equiv \bar{\mu}/\rho a$ increases the aperiodic region, and in the damped oscillatory region increases the oscillation frequency as well as the decay magnitude.

It may be mentioned here that, for higher liquid height ratio h/a , the theory presented here will yield only approximate values. This is due to the fact that the liquid motion penetrates only below the membrane surface to a depth of about one wavelength, while the lower part of the liquid will remain mainly at rest. For low liquid ratio $h/a \leq 0.5$ these results, satisfying all bottom-adhesive conditions, and only the normal side-wall condition (showing only a small side-wall area), yield good results. For large height ratio $h/a > 0.5$, the contribution of the adhesive condition at the side-wall will contribute the major part of the damping. For such cases a new method is being developed at the present time and will be presented in due course.

For the case with a cover plate the above procedure will be similar.

REFERENCES

- BALENDRA, T., ANG, K. K., PARAMASIVAM, P. & LEE, S. L. 1982 Free vibration analysis of cylindrical liquid storage tanks. *International Journal of Mechanical Science* **24**, 47–59.
- BARON, M. L. & SKALAK, R. 1962 Free vibrations of fluid-filled cylindrical shells. *Proceedings of ASCE* **88**, 17–43.
- BAUER, H. F. 1970 Hydroelastische Schwingungen im aufrechten Kreiszyylinderbehälter. *Zeitschrift für Flugwissenschaften* **18**, 117–134.
- BAUER, H. F. 1973 Hydroelastische Schwingungen in einem starren Kreiszyylinder bei elastischer Flüssigkeitsoberflächenabdeckung. *Zeitschrift für Flugwissenschaften* **21**, 202–213.
- BAUER, H. F. 1981 Hydroelastic vibrations in a rectangular container. *International Journal of Solids and Structures* **17**, 639–652.
- BAUER, H. F. 1987 Hydroelastic oscillations of a viscous infinitely long liquid column. *Journal of Sound and Vibration* **119**, 249–265.
- BAUER, H. F. 1995 Coupled frequencies of a liquid in a circular cylindrical container with elastic liquid surface cover. *Journal of Sound and Vibration* **180**, 689–704.

- BAUER, H. F. & EIDEL, W. 1997a Axisymmetric viscous liquid oscillations in a cylindrical container. *Forschung im Ingenieurwesen* **63**, 189–201.
- BAUER, H. F. & EIDEL, W. 1997b Oscillations of a viscous liquid in a cylindrical container. *Aerospace Science and Technology* **8**, 519–532.
- BAUER, H. F., HSU, T. M. & WANG, J. T. S. 1968a Interaction of a sloshing liquid with elastic containers. *ASME, Journal of Basic Engineering* **90**, 373–377.
- BAUER, H. F. & SIEKMANN, J. 1969 Note on linear hydroelastic sloshing. *Zeitschrift für Angewandte Mathematik und Mechanik* **49**, 577–589.
- BAUER, H. F. & SIEKMANN, J. 1971 Dynamic interaction of a liquid with the elastic structure of a circular cylindrical container. *Ingenieur Archiv* **40**, 266–280.
- BAUER, H. F., SIEKMANN, J. & WANG, J. T. S. 1968b Axisymmetric hydroelastic sloshing in an annular cylindrical container. *Journal of Spacecraft and Rockets* **5**, 981–983.
- BAUER, H. F., WANG, J. T. S. & CHEN, P. Y. 1972 Axisymmetric hydroelastic sloshing in a circular cylindrical container. *Aeronautical Journal* **76**, 704–712.
- BHUTA, P. G., PRAVIN, G. & KOVAL, L. R. 1964 Coupled oscillations of a liquid with a free surface in a tank. *Zeitschrift für Angewandte Mathematik und Physik* **15**, 466–480.
- BHUTA, P. G. & KOVAL, L. R. 1964 Hydroelastic solution of the sloshing of a liquid in a cylindrical tank. *Journal of the Acoustical Society of America* **36**, 2071–2079.
- CHU, W.-H. 1963 Breathing vibrations of a partially filled cylinder tank-linear theory. *Journal of Applied Mechanics* **30**, 532–536.
- HAROUN, M. A. & HOUSNER, G. W. 1981 Earthquake response of deferrable liquid storage tanks. *Journal of Applied Mechanics* **48**, 411–418.
- JAIN, R. K. 1974 Vibration of fluid-filled, orthotropic cylindrical shells. *Journal of Sound and Vibration* **37**, 379–388.
- LAKIS, A. A. & PAIDOUSSIS, M. P. 1971 Free vibration of cylindrical shells partially filled with liquid. *Journal of Sound and Vibration* **19**, 1–15.
- LEISSA, A. W. 1969 *Vibration of Plates* (NASA-SP-160). Washington, D.C.: U.S. Government Printing Office.
- LINDHOLM, U. S., KANA, D. D. & ABRAMSON, H. N. 1962 *Journal of Aerospace Sciences* **29**, 1052–1059. Breathing vibrations of a circular cylindrical shell with an internal liquid.
- MILES, J. W. 1958 On the sloshing of liquid in a flexible tank. *Journal of Applied Mechanics* **25**, 277–283.
- NASH, W. A., SHAABAN, S. H. & MONZAKIS, T. 1980 Response of liquid storage tanks to seismic motion. In *Proceedings of the Third IUTAM Symposium on Shell Theory*, pp. 393–403. Amsterdam: North-Holland.
- SALEME, E. & LIBER, T. 1965 Breathing vibrations of pressurized partially filled tanks. *AIAA Journal* **3**, 132–136.
- STILLMAN, W. E. 1973 Free vibration of cylinders containing liquid. *Journal of Sound and Vibration* **30**, 509–524.
- TSUI, T. Y. & SMALL, N. C. 1968 Hydroelastic oscillations of a liquid surface in an annular circular cylindrical tank with flexible bottom. *Journal of Spacecraft and Rockets* **5**, 202–206.
- YAMAKI, N., TANI, J. & YAMAJI, T. 1984 Free vibration of a clamped-clamped circular cylindrical shell partially filled with liquid. *Journal of Sound and Vibration* **94**, 531–550.

APPENDIX A: UNCOUPLED FREQUENCIES

A.1. MEMBRANE FREQUENCY

Solving the uncoupled membrane equation (3a) we obtain the natural frequencies

$$\omega_{mn}^{(m)} = \frac{\bar{\epsilon}_{mn}}{a} \sqrt{\frac{T}{\mu}}, \quad m = 0, 1, 2, \dots, n = 1, 2, 3, \dots,$$

where $\bar{\epsilon}_{mn}$ are the roots of $J_m(\bar{\epsilon}_{mn}) = 0$. This, for reasons of comparison with the coupled frequencies $\omega^* = \omega a^2/\nu$, yields,

$$\omega_{mn}^{*(m)} = \bar{\epsilon}_{mn} \sqrt{\frac{T^*}{\mu^*}}.$$

For the circular plate the natural frequencies are

$$\omega_{mn}^{(p)} = \frac{\lambda_{mn}^2}{a^2} \sqrt{\frac{D}{\mu}},$$

where λ_{mn} are the eigenvalues. This yields

$$\omega_{mn}^{*(p)} = \lambda_{mn}^2 \sqrt{\frac{D^*}{\mu^*}}, \quad m = 0, 1, 2, \dots, n = 1, 2, 3, \dots$$

In the case of a *clamped* plate, the eigenvalues λ_{mn} are obtained from

$$J_m(\lambda)I_{m+1}(\lambda) + I_m(\lambda)J_{m+1}(\lambda) = 0$$

and are presented in the form of a table for $n = 1, 2, \dots$ and $m = 0, 1, 2, \dots$ in Bauer (1995).

For a *simply supported* plate, λ_{mn} is obtained from the expression

$$J_{m+1}(\lambda)I_m(\lambda) + I_{m+1}(\lambda)J_m(\lambda) - \frac{2\lambda}{(1-\bar{\nu})} J_{m+1}(\lambda)I_m(\lambda) = 0,$$

while for a *free* plate it is obtained from

$$\frac{\lambda^2 J_m(\lambda) + (1-\bar{\nu})[\lambda J'_m(\lambda) - m^2 J_m(\lambda)]}{\lambda^2 I_m(\lambda) - (1-\bar{\nu})[\lambda I'_m(\lambda) - m^2 I_m(\lambda)]} = \frac{\lambda^3 J'_m(\lambda) + m^2(1-\bar{\nu})[\lambda J'_m(\lambda) - J_m(\lambda)]}{\lambda^3 I'_m(\lambda) - m^2(1-\bar{\nu})[\lambda I'_m(\lambda) - I_m(\lambda)]}$$

For a *guided* plate, λ_{mn} is obtained from

$$2\lambda^3 I'_m(\lambda)J'_m(\lambda) + m^2(1-\bar{\nu})[I_m(\lambda)J'_m(\lambda) - I'_m(\lambda)J_m(\lambda)] = 0,$$

and for an *elastically supported* plate the equation to be solved is

$$\begin{aligned} & \left\{ [J_{m+2}(\lambda) - J_{m-2}(\lambda)] - \frac{2}{\lambda} \left(\bar{\nu} + \frac{Ka}{D} \right) [J_{m+1}(\lambda) - J_{m-1}(\lambda)] + \left(2 + \frac{4m^2\bar{\nu}}{\lambda} \right) J_m(\lambda) \right\} \\ & \times \left\{ [I_{m+3}(\lambda) + I_{m-3}(\lambda)] + \frac{2}{\lambda} [I_{m+2}(\lambda) + I_{m-2}(\lambda)] + \left[3 - \frac{4}{\lambda^2} - 4(2-\bar{\nu}) \frac{m^2}{\lambda^2} \right] \right. \\ & \times [I_{m+1}(\lambda) + I_{m-1}(\lambda)] + \frac{4}{\lambda^3} [2m^2(2-3\bar{\nu}) + \lambda^2] I_m(\lambda) \left. \right\} \\ & - \left\{ [I_{m+2}(\lambda) + I_{m-2}(\lambda)] + \frac{2}{\lambda} \left(\bar{\nu} + \frac{Ka}{D} \right) [I_{m+1}(\lambda) + I_{m-1}(\lambda)] + \left(2 - \frac{4m^2\bar{\nu}}{\lambda} \right) I_m(\lambda) \right\} \\ & \times \left\{ \frac{2}{\lambda} [J_{m+2}(\lambda) - J_{m-2}(\lambda)] - [J_{m+3}(\lambda) - J_{m-3}(\lambda)] + \left[3 + \frac{4}{\lambda^2} + 4(2-\bar{\nu}) \frac{m^2}{\lambda^2} \right] \right. \\ & \times [J_{m+1}(\lambda) - J_{m-1}(\lambda)] + \frac{4}{\lambda^3} [2m^2(2-3\bar{\nu}) - \lambda^2] J_m(\lambda) \left. \right\} = 0. \end{aligned}$$

For reasons of comparison one could write $Ka/D \equiv K^*/D^*$, where $K^* \equiv K/\rho v^2$ and $D^* \equiv D/\rho v^2 a$.

A.2. SLOSHING FREQUENCY

The uncoupled natural frequencies of the liquid are given by

$$\omega_{mn}^{2(l)} = \frac{g\epsilon_{mn}}{a} \tanh\left(\epsilon_{mn} \frac{h}{a}\right), \quad m = 0, 1, 2, \dots, \quad n = 1, 2, \dots,$$

where ε_{mn} are the roots of $J'_m(\varepsilon_{mn}) = 0$. This could also be written as

$$\omega_{mn}^{*2(l)} = g^* \varepsilon_{mn} \tanh\left(\varepsilon_{mn} \frac{h}{a}\right).$$

APPENDIX B: NOMENCLATURE

$A(z), C(z), D(z)$	coefficients of equation (8)
$A_{1mn} - A_{4mn}$	coefficients in equation (11)
a	radius of tank
D	flexural rigidity of plate
D^*	$\equiv D/\rho v^2 a$
E	Young's modulus of plate
g	gravitational acceleration
g^*	$\equiv ga^3/v^2$
h	liquid height
I_m	modified Bessel function of order m
i	imaginary unit
J_m	Bessel function of the first kind of order m
K	distributed stiffness of plate
K^*	$\equiv K/\rho v^2$
M_r	moment
P_0^*	constant
p	pressure
p_0	static pressure
r, φ, z	coordinate system
S	$\equiv sa^2/v$
s	characteristic index
T	tension of membrane
T^*	$\equiv Ta/\rho v^2$
t	time
u, v, w	velocity components of liquid
U_m, V_m, W_m	coefficients
V_r	shearing force
α	parameter $\alpha^2 \equiv (\mu^* S^2 + g^*)/D^*$
β	parameter $\beta^2 \equiv (\mu^* S^2 + g^*)/T^*$
δ	plate thickness
ε_{mn}	roots of $J'_m(\varepsilon) = 0$
$\bar{\varepsilon}_{mn}$	roots of $J_m(\bar{\varepsilon}) = 0$
$\bar{\eta}$	dynamic viscosity of liquid
λ	wavelength
λ_{mn}	eigenvalue of circular plate
μ_{mn}	parameter defined by equation (10)
$\bar{\mu}_{mn}$	parameter $= a\mu_{mn}$
$\bar{\mu}$	mass/unit area of membrane or plate
μ^*	$\equiv \bar{\mu}/\rho a$
v	$\equiv \bar{\eta}/\rho$
$\bar{\nu}$	Poisson ratio of plate
ζ, η, ζ	displacement components of membrane or plate
ρ	density of liquid
σ	surface tension
σ^*	$\equiv \sigma a/\rho v^2$
ϕ, ψ	defined by equation (5a)
$\omega_{mn}^{(p)}$	uncoupled natural frequency of circular plate
$\omega_{mn}^{(l)}$	uncoupled natural frequency of liquid
$\omega_{mn}^{(m)}$	uncoupled natural frequency of membrane
$\omega_{mn}^{*(m)}$	uncoupled natural frequency of membrane